Enhanced light transmission through a single subwavelength aperture

Tineke Thio, K. M. Pellerin, and R. A. Linke

NEC Research Institute, 4 Independence Way, Princeton, New Jersey 08540

H. J. Lezec and T. W. Ebbesen

Institut de Science et d'Ingéniérie Supramoléculaires, Université Louis Pasteur, 4 Rue B. Pascal, 67000 Strasbourg, France

Received July 9, 2001

The optical transmission through a subwavelength aperture in a metal film is strongly enhanced when the incident light is resonant with surface plasmons at the corrugated metal surface surrounding the aperture. Conversely, the aperture acts as a novel probe of the surface plasmons, yielding useful insights for optimizing the transmission enhancement. For the optimal corrugation geometry, a set of concentric circular grooves, three times more light is transmitted through the central subwavelength aperture than directly impinges upon it. This effect is useful in the fabrication of near-field optical devices with extremely high optical throughput. © 2001 Optical Society of America

OCIS codes: 230.3990, 240.6680, 180.5810, 210.0210.

The usefulness of near-field optical devices,[1] which owe their extremely high resolution to the presence of an aperture of size $d \ll \lambda$, where λ is the optical wavelength, is limited by their extremely low transmission efficiencies.[2] Transmission T of a subwavelength aperture in an ideal-metal sheet, normalized to the area of the aperture, is predicted[3] to follow the formula $T/f \sim (d/\lambda)$.[4] A large transmission enhancement is observed when the metal surface surrounding the aperture has periodic corrugations,[4,5] which permit grating coupling of the incident light with surface plasmon (SP) modes at the metal surface.[6–8] At resonance, a large enhancement of the oscillating electric field at the hole causes the transmission to be unusually high despite the fact that the propagation of light through the subwavelength hole is evanescent.[9] The transmission enhancement can have a large effect on such fields as near-field microscopy and high-density data storage.[5]

Conversely, the single aperture acts as a novel probe of the SP modes on the metal surface, elucidating the properties of the SP and allowing us to tailor the surface corrugation to maximize enhancement factor F_{SP}, the ratio of the transmission of a single hole with and without surface corrugation. We find the highest F_{SP} for a set of concentric circular grooves surrounding the hole with depth $h \approx 75$ nm.

The structures that we study here were fabricated in a free-standing Ni film[10] of thickness 300 nm, coated on one side with a 100-nm Ag layer. We used a Micrion Model 9500 focused ion beam machine (5-nm resolution) to mill a single circular aperture, surrounded by surface topography on the Ni side (Fig. 1, insets); the corrugation depth was determined by normalizing to the ion dose required for milling through the thickness of the metal film. Subsequently a 30-nm layer of Ag was rf sputtered over the Ni surface.[10] Transmission spectra were measured with illumination from a tungsten halogen lamp system at normal incidence and with a divergence less than 3°.

Figure 1(A) shows T/f of a single hole ($d = 440$ nm) surrounded by a set of concentric circular grooves

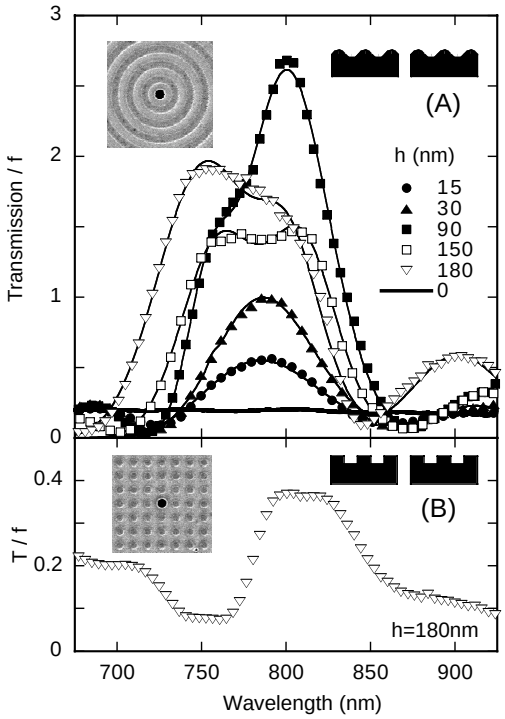

Fig. 1. Transmission spectra of a single aperture ($d = 440$ nm) surrounded by (A) rings with sinusoidal cross section and (B) a square array of dimples ($h = 180$ nm). Left insets, focused ion beam images of typical samples; right insets, cross sections of the hole and corrugation. Illumination is on the corrugated surface. Thin solid curves are fits to the data.

0146-9592/01/241972-03$15.00/0

(left-hand inset) with mean radii $R_k = kP$ ($P = 750$ nm, $k = 1, 2, \ldots, 10$). The grooves have a sinusoidal profile (right-hand inset) with peak-to-peak amplitude h. The transmission is enhanced at two wavelengths near $\lambda \approx P$ relative to that of a bare aperture ($h = 0$). At the peak, $T/f \approx 3$, three times more light is transmitted through the hole than is directly impinging upon it. In addition, there is a weaker peak at $\lambda \approx 900$ nm. For illumination on the uncorrugated side (not shown), F_{SP} is reduced by nearly a factor of 10.

The peak transmission shown in Fig. 1(A) is larger, by a factor of ~8, than that of a single hole with a square array of dimples with lattice constant $P = 750$ nm [Fig. 1(B)]. This is so because, for randomly polarized light such as that used in these experiments, the circularly symmetric Huygens waves emerging from the aperture are better matched to the SP modes of the rings than to those of the square array.[6]

Furthermore, the well-developed Wood anomaly[11–13] minimum at $\lambda \approx 750$ nm [Fig. 1(B)], similar to the deep minima seen in the spectra of square lattices of holes,[4,6,10] is altogether absent for the ring corrugation [Fig. 1(A)], where for normal incidence the diffraction is distributed evenly over 2π of the azimuthal angle. In the square-symmetry case [Fig. 1(B)] the diffracted intensity is concentrated into four well-defined directions, each with a narrow distribution of k-vectors. In the Rayleigh formulation,[14,15] it is this coherent interference that leads to a divergence in the intensity of the diffracted beam and consequently to a minimum in the zero-order transmission.

The transmission spectra of Fig. 1(A) thus reflect the true response of the surface plasmons, undistorted by the Rayleigh minima. We fitted the transmission resonances of Fig. 1(A) to a sum of three Gaussians of the form $T/f = A_i \exp\{-[(E - E_i)/\Delta E_i]^2\}$, with the central photon energy E_i (or the resonant wavelength $\lambda_i = hc/E_i$), amplitude A_i, and width ΔE_i of each of the three resonant peaks ($i = 1, 2, 3$) as fitting parameters. The thin solid curves through the data of Fig. 1(A) show that the fits are excellent. All three resonances are associated with SP modes of the corrugated surface: None is present when $h = 0$. The mode at $\lambda_3 \approx 900$ nm is likely to correspond to a mode of the circularly symmetric grooves. Slits[16] and grooves[17] in metallic films have a rich spectral structure owing to the presence of modes inside each slit as well as to interactions between the slits.

The resonance wavelengths λ_1, $\lambda_2 \approx P$ are similar for square-wave and sinusoidal profiles [Fig. 2(A)]: $\lambda_1 \approx 760$ nm, nearly independently of h, whereas λ_2 is longer and increases slightly with h. A double resonance is predicted for the transmission of a metal film with surface topography on both sides.[9,18,19] But in our samples only one of the two surfaces is corrugated, and here the double resonance indicates the presence of a gap at a level crossing of the SP dispersion. Physically, the incident light excites standing waves of charge displacement at the metal surface. There are two such standing-wave modes, which are nearly degenerate in energy, however with different distributions of the electromagnetic fields. In what follows, we present a real-space model of the SP modes, which gives valuable insight into maximizing F_{SP}.

Figure 3 illustrates, for a corrugation with square-wave cross section, the surface charge displacements and the electric fields associated with the two SP modes. For mode 1 the charge displacement is confined to the in-plane surface of the metal, along the ridges and within the valleys; one expects that $\lambda_1 \approx \lambda_{h=0} = \mathrm{P}[\epsilon_m \epsilon_d/(\epsilon_m + \epsilon_d)]^{1/2} = n_{\mathrm{eff}} P$, where n_{eff} is an effective refractive index determined by ϵ_m and ϵ_d, the dielectric constants of the metal and the adjacent dielectric, respectively.[6] Indeed, we observe [Fig. 2(A)] that $\lambda_1 \approx \lambda_{h=0} = 763$ nm. For mode 2, however, the charge displacement occurs between ridges and valleys of the grooves, and most of the electromagnetic fields reside in the grooves or dimples, in close vicinity to the metallic walls, so n_{eff} is larger than for mode 1, and $\lambda_2 > \lambda_1$. A linear dependence of the SO anticrossing gap found[20] for small h is not expected to hold for our sample, for which h is large ($0.13 < 2\pi h/P < 1.5$).

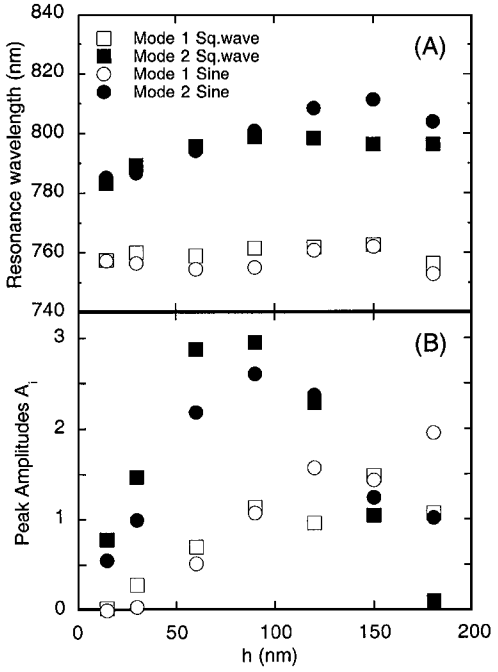

Fig. 2. (A) Resonance wavelengths and (B) amplitude of SP mode 1 and SP mode 2 for square-wave (Sq. wave) and sinusoidal (Sine) cross sections.

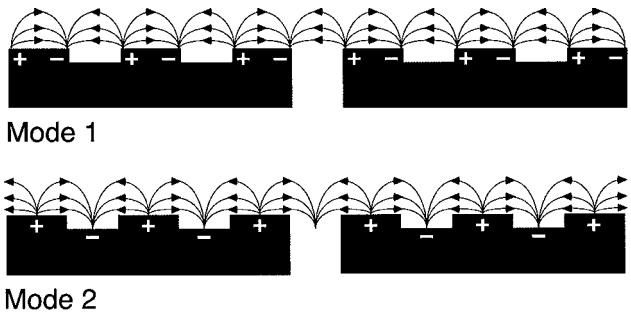

Fig. 3. Real-space model of charge displacement at the metal surface and associated electric fields of SP modes at level crossing.

The electric field lines of the SP modes indicate (Fig. 3) that for mode 1 the electromagnetic fields are most intense at the edges of the ridges, whereas for mode 2 they are maximal at the centers of both the ridges and the grooves and at the center of the aperture as well. For this reason one expects mode 2 to give stronger coupling between the front and back sides of the metal film, and therefore a larger F_{SP}. Indeed, we measure $A_2 \approx 4A_1$ at small h [Fig. 2(B)].

A_1 saturates at $h \approx 90$ nm, but A_2 decreases for $h >$ 90 nm, becoming vanishingly small near $h \approx 180$ nm. This can be understood in terms of our model: For mode 1 the in-plane oscillating current occurs independently of the depth of the grooves, whereas for mode 2 the charge displacement into and out of the grooves is no longer longitudinal with respect to the wave vector, and the coupling to the incident light is diminished. Stated simplistically, when the grooves become deep, no charge flows into them; for this reason A_2 decreases with h at large h. The crossover depth for both modes, $h \approx 90$ nm, is 3–4 times the skin depth in this wavelength range,[10] consistent with the surface nature of the SP modes. In through holes or slits, the ultimate limit of large h, calculations[9,21] show only mode 1.

F_{SP} is highest when the width of the grooves is approximately half of the pitch and is roughly equal for corrugations with sinusoidal cross section and for those with square-wave cross section. Because the exact profile is not important, the fabrication of enhanced devices is robust to such effects as rounding of the surface features.

Finally, we measured the diameter dependence of F_{SP} for a ring corrugation with a sinusoidal profile and $h = 150$ nm. For all d, the shape of the spectrum is the same as that for $d = 440$ nm [squares in Fig. 1(A)]. At the peak wavelength, $\lambda_2 = 800$ nm, $T/f \approx 1.5$ independently of d; i.e., the total transmitted power is proportional to the area of the hole. Comparing the enhanced transmission with the transmission of a reference series of bare apertures fabricated in the same film, we find that $F_{SP} \sim 1/d^2$. At $d = 200$ nm ($d/\lambda = 0.25$), $F_{SP} = 50$ even though $h = 150$ nm is not optimal. An extrapolation of our data suggests that in principle $F_{SP} \approx 1600$ can be achieved at $h \approx 75$ nm for a 50-nm aperture.

To summarize, we have presented a systematic study of enhanced transmission through single holes in a metal film as a function of corrugation geometry. The optimal geometry is a circular corrugation, periodic in the radial direction, with $h \approx 75$ nm. In such a structure, Wood's anomaly is absent and an anticrossing in the SP dispersion at $\lambda \approx P$ is revealed by a double resonance in the transmission spectrum. Our real-space model for the two SP modes accounts for the rich corrugation geometry dependence of the transmission spectra and points the way for further optimization of the transmission enhancement. The high transmission efficiencies deep in the subwavelength region hold great promise for the use of these enhanced devices in near-field optical microscopies and ulrtahigh-density optical data storage. The ability to tune the resonant wavelength[6] makes the devices extremely flexible for system integration.

T. Thio's e-mail address is tineke@research.nj.nec.com.

References

1. B. Heckt, B. Sick, U. P. Wild, V. Deckert, R. Zenobi, O. J. F. Martin, and D. W. Pohl, J. Chem. Phys. **112,** 7761 (2000).
2. E. Betzig, J. K. Trautman, T. D. Harris, J. S. Weiner, and R. L. Kostelak, Science **251,** 1468 (1991).
3. H. A. Bethe, Phys. Rev. **66,** 163 (1944).
4. T. W. Ebbesen, H. J. Lezec, H. F. Ghaemi, T. Thio, and P. A. Wolff, Nature **391,** 667 (1998).
5. D. E. Grupp, H. J. Lezec, T. Thio, and T. W. Ebbesen, Adv. Mater. **11,** 860 (1999).
6. H. F. Ghaemi, T. Thio, D. E. Grupp, T. W. Ebbesen, and H. J. Lezec, Phys. Rev. B **58,** 6779 (1998).
7. R. H. Ritchie, Phys. Rev. **106,** 874 (1957).
8. H. Raether, *Surface Plasmons on Smooth and Rough Surfaces and on Gratings*, Vol. 111 of Springer Tracts in Modern Physics (Springer-Verlag, Berlin, 1988).
9. L. Martín-Moreno, F. J. García-Vidal, H. J. Lezec, K. M. Pellerin, T. Thio, J. B. Pendry, and T. W. Ebbesen, Phys. Rev. Lett. **86,** 1114 (2001).
10. D. E. Grupp, H. J. Lezec, K. M. Pellerin, T. W. Ebbesen, and T. Thio, Appl. Phys. Lett. **77,** 1569 (2000).
11. R. W. Wood, Philos. Mag. **4,** 396 (1902).
12. R. W. Wood, Phys. Rev. B **48,** 928 (1935).
13. U. Fano, J. Opt. Soc. Am. **31,** 213 (1941).
14. Lord Rayleigh, Proc. R. Soc. London Ser. A **79,** 399 (1907).
15. Lord Rayleigh, Philos. Mag. **14,** 60 (1907).
16. J. A. Porto, F. J. García-Vidal, and J. B. Pendry, Phys. Rev. Lett. **83,** 2845 (1999).
17. W.-C. Tan, T. W. Preist, J. R. Sambles, and N. P. Wanstall, Phys. Rev. B **59,** 12661 (1999).
18. W.-C. Tan, T. W. Preist, and J. R. Sambles, Phys. Rev. B **62,** 11134 (2000).
19. U. Schröter and D. Heitmann, Phys. Rev. B **60,** 4992 (1999).
20. W. L. Barnes, T. W. Preist, S. C. Kitson, and J. R. Sambles, Phys. Rev. B **54,** 6227 (1996).
21. U. Schröter and D. Heitmann, Phys. Rev. B **58,** 15419 (1998).